

# Geophysical Research Letters

## RESEARCH LETTER

10.1029/2020GL090217

### Key Points:

- ARTEMIS observes lunar ions in the terrestrial magnetotail lobes
- Observations of lunar ions provide a useful tool to estimate the plasma convection in the lobes
- The inferred convection in the tail lobes is correlated with upstream solar wind parameters and magnetospheric activity

### Correspondence to:

X. Cao,  
xin-cao@uiowa.edu

### Citation:

Cao, X., Halekas, J. S., Chu, F., Kistler, M., Poppe, A. R., & Glassmeier, K.-H. (2020). Plasma convection in the terrestrial magnetotail lobes measured near the Moon's orbit. *Geophysical Research Letters*, 47, e2020GL090217. <https://doi.org/10.1029/2020GL090217>

Received 12 AUG 2020

Accepted 2 OCT 2020

Accepted article online 7 OCT 2020

## Plasma Convection in the Terrestrial Magnetotail Lobes Measured Near the Moon's Orbit

Xin Cao<sup>1</sup> , Jasper S. Halekas<sup>1</sup> , Feng Chu<sup>1</sup> , Michael Kistler<sup>1</sup>, Andrew R. Poppe<sup>2</sup> , and Karl-Heinz Glassmeier<sup>3</sup> 

<sup>1</sup>Department of Physics and Astronomy, University of Iowa, Iowa City, IA, USA, <sup>2</sup>Space Sciences Laboratory, University of California, Berkeley, CA, USA, <sup>3</sup>Institut für Geophysik und Extraterrestrische Physik, Technische Universität Braunschweig, Braunschweig, Germany

**Abstract** In order to study the plasma convection in the deep magnetotail lobes near lunar orbit, we investigated ions originating from the tenuous exosphere and surface of the Moon, which are measured by the Acceleration, Reconnection, Turbulence, and Electrodynamics of Moon's Interaction with the Sun (ARTEMIS) spacecraft. Directly measuring the plasma convection in the tail lobes is difficult, due to the typically large positive spacecraft potential. In this work we show that in the terrestrial magnetotail near the Moon, the convection velocity can be estimated by measuring the velocity of lunar ions. Determining what factors control the lobe convection is important in understanding the linkage between the upstream conditions and the dynamics of the tail lobes. Based on systematic analysis of multiple ARTEMIS observations and OMNI data, we find that the interplanetary magnetic field (IMF) and magnetospheric activity plays an important role in controlling plasma convection in the near-Moon lobes.

**Plain Language Summary** Studying the plasma convection is important for us to understand the magnetospheric dynamics. We used the Acceleration, Reconnection, Turbulence, and Electrodynamics of Moon's Interaction with the Sun spacecraft to investigate the convection pattern in the terrestrial magnetotail lobes near the Moon's orbit, by analyzing the motion of lunar ions. Combined with the solar wind data and the magnetospheric activity index, we found that the magnetospheric convection near the Moon's orbit may be influenced by the upstream solar wind. This technique provides a useful method to estimate the plasma motion in a tenuous space environment.

## 1. Introduction

Recent studies show that a tenuous exosphere exists around the Moon, the majority of which is composed of neutral particles released from the lunar surface via micrometeorite impact (Halekas et al., 2011, 2012, 2013; Hartle & Killen, 2006; Horányi et al., 2015), solar wind sputtering, and thermal and chemical release (Cook et al., 2013; Sarantos, Killen, et al., 2012; Stern, 1999; Vorburger et al., 2014). These neutral particles can be naturally transformed to heavy ions with the same mass through multiple processes, including photoionization, charge exchange, and electron impact ionization (Huebner & Mukherjee, 2015; McGrath et al., 1986; Sarantos, Hartle, et al., 2012). Studying the behavior of lunar ions in the magnetotail lobes can help us understand linkages between the lunar surface, the exosphere, and the dynamics of the tail lobes.

The ambient plasma density when the Moon orbits through regions such as the solar wind, the magnetospheric plasma sheet, or the magnetosheath is much higher than that of the lunar ions (Halekas et al., 2011). In contrast, in the terrestrial magnetotail lobes, the background flow is sub-Alfvénic, and the density of lunar ions is commonly comparable to or even larger than that of the ambient lobe plasma (Halekas et al., 2018). Therefore, the magnetotail lobes provide a unique environment to study the dynamics of the lunar ions. In this scenario, Zhou et al. (2013) inferred that the average mass of lunar pickup ions was ~28 amu, based on the plasma quasi-neutrality requirement and the underestimation of the ion density by the non-mass resolving Acceleration, Reconnection, Turbulence, and Electrodynamics of Moon's Interaction with the Sun (ARTEMIS) instruments. Cao et al. (2020) showed that the acceleration of lunar ions in the tail lobes could be predominantly driven by magnetic tension and pressure forces by analyzing the ARTEMIS data combined with a magnetic force model. During this process, the lunar ions are coupled to the ambient plasma convection in the tail lobes by the mass loading effect. Therefore, measurement of the behavior of lunar ions can be

used to estimate the plasma convection in the deep magnetotail lobes. In contrast, the ambient convection velocity is typically not directly measurable by ARTEMIS, due to the large positive spacecraft potential in the low-density lobe regions (Poppe et al., 2012).

The plasma convection in the tail lobes has been shown to have opposite lateral patterns in the northern and southern lobes at  $\sim 10-R_E$  downtail (Haaland et al., 2008, 2009). In both lobes, the plasma tends to move toward the central plasma sheet. The magnitude of the convection velocity is affected by the upstream solar wind conditions, for example, solar wind dynamic pressure, the interplanetary magnetic field (IMF), and its clock angle, and the magnetospheric activity, for example, Dst index (disturbance storm time). Specifically, the dawn-dusk convection in different lobes strongly depends on the dawn-dusk component of the IMF direction. Ohma et al. (2019) showed that the magnitude of the asymmetry of the convection flow could also be affected by tail reconnection, which is linked to magnetospheric activity. McCoy et al. (1975) and Lin et al. (1977) showed the magnitude of field lines in the magnetotail lobes moving toward the plasma sheet could be  $\sim 15$  km/s typically in the Apollo era. Troshichev et al. (1999) revealed that the total of plasma and magnetic pressure are balanced between the lobe regions and plasma sheet by studying the convection in the distant tail region far beyond the orbit of the Moon.

In this paper, we investigated events during which the ARTEMIS spacecraft flew by the dayside of the Moon and observed lunar ions in the deep magnetotail lobes ( $\sim 60 R_E$ ), and analyzed their relationship with upstream solar wind conditions and magnetospheric activity. The midtail region near the Moon's orbit is the transitional region linked the near tail and distant tail. Studying the dynamics of this tail region can help us to understand the magnetospheric activity across through the whole tail region, for example, the substorms, the tail reconnection, the plasmoids, and the magnetic and plasma fluctuations. The correlation of the lobe plasma convection velocity inferred from the lunar ions with upstream solar wind conditions and magnetospheric activity indicates that the upstream environment plays an important role in the plasma convection of the deep magnetotail lobes.

## 2. Near-Lunar and Upstream Observations

The ARTEMIS mission includes two spacecraft, which were redeployed from the five spacecraft of the Time History of Events and Macroscale Interactions during Substorms (THEMIS) mission (Angelopoulos, 2011). The two redeployed spacecraft were renamed ARTEMIS P1 and P2 and transferred into the orbit around the Moon in mid-2011. The orbits of the two probes are elliptical and nearly equatorial. The data utilized in this study are measured by two of the onboard instruments: ESA and FGM. The ESA measures the ion distribution from a few eV to 25 keV and the electron distribution from a few eV up to 30 keV (McFadden et al., 2008). The FGM measures the vector magnetic field at up to 64 Hz (Auster et al., 2008). The coordinate system utilized in this study is Selenographic Solar Ecliptic (SSE), in which the  $+X_{SSE}$  axis is defined to be oriented toward the Sun from the center of the Moon, the  $+Z_{SSE}$  axis is oriented toward the ecliptic north pole, and the  $+Y_{SSE}$  axis completes the right-handed system. A dominant positive or negative  $B_x$  component was observed during the events, which indicates that the Moon was in the north or south tail lobe respectively. The solar wind and Dst index data can be obtained from NASA's OMNI data set (King & Papitashvili, 2005). The coordinate system utilized for the OMNI data is Geocentric Solar Ecliptic (GSE), which is approximately identical to SSE for vector quantities in the deep magnetotail lobes.

As discussed by Cao et al. (2020), the heavy ion velocity is smaller than the nominal ion velocity measured by ARTEMIS by a factor of approximately  $\sqrt{M}$  (where  $M$  is the atomic mass) in the tenuous magnetotail lobes, since the ESA measures flux as a function of energy per charge, but does not discriminate between ions of different mass. (The nominal ion velocity was measured under the proton-only assumption). The ion density is thus underestimated by a factor of  $\sqrt{M}$  since the particle flux is correctly measured regardless of ion mass (McFadden et al., 2008; Zhou et al., 2013). Zhou et al. (2013) found the average mass to be 28 amu in the tail lobes. We therefore utilize a correction factor of  $\sqrt{M} = \sqrt{28} \approx 5.29$ . To measure the lunar ion velocity moment accurately, background noise must be excluded, since it would affect the measurement of the lunar ion velocity. The moments of lunar ions are therefore calculated by restricting the energy range to that containing lunar ions. Since the mass loading effect couples the lunar ions to the ambient plasma convection (Cao et al., 2020), the motion of lunar ions serves as an approximate tracer of the convection patterns in the tail lobes.

In general, the magnetospheric dynamics are influenced by the upstream interactions with the solar wind. Figure 1 illustrates the measurements of lunar ions and ambient magnetic field by ARTEMIS and the synchronous measurement of upstream conditions from the OMNI data set. We checked 30 min prior to each event, which indicated quasi-quiet solar wind parameters during these events. All solar wind data are sampled with 1-min time resolution, while the Dst index is sampled with 1-hr time resolution. The Dst index in the OMNI data set is provided by the World Data Center for Geomagnetism. Panels (a)–(f) show the three components of the lunar ion velocity and the ambient magnetic field measured by ARTEMIS, and panels (g)–(l) show six different parameters of upstream conditions obtained from OMNI data set. Panel (a) reveals that the lunar ions move with a velocity of a few kilometer per second upward from the Moon's surface, likely due to the outward electric field in the near-surface plasma sheath. During this process, lunar ions experience parallel acceleration along the ambient magnetic field in the lobes (Poppe et al., 2012). Panel (b) shows that lunar ions during some events move toward the +Y direction and others toward the –Y direction, which indicates the direction of the dawn-dusk convection flow in the magnetotail lobes (Haaland et al., 2008). This convection pattern has been suggested to be produced by the asymmetric pressure distribution caused by different mechanisms in open and closed magnetospheres, which result from the magnetospheric interaction with the upstream solar wind (Cowley, 1981; Cowley & Lockwood, 1992; Khurana et al., 1996; Ohma et al., 2019; Tenfjord et al., 2015). Panel (c) shows that the lunar ion velocities far from the Moon surface are primarily northward for three events, in contrast to the predominately southward lunar ion velocity in the other 13 events. The events with northward convection velocity occur during orbits with a negative  $B_x$  component of the ambient magnetic field, as panel (d) shows. This indicates that lobe plasma in both the northern and southern lobes predominantly moves toward the central plasma sheet, as expected. Panel (e) reveals that the lobe  $B_y$  component seems consistent with the lunar ion  $V_y$  component, possibly because the lateral component of the ambient magnetic field is perturbed by the mass loading effect of lunar ions. Panel (g) shows that two of the highest solar wind dynamic pressure events are in the southern lobes, compared to the medium or low dynamic pressure in other events. Panels (h) and (i), respectively, show the Y component of the solar wind electric field ( $E_y$ ) and the Dst index. Two of the three events in the southern lobe (those which were furthest from the Moon surface) show negative IMF  $B_y$  values. Consistent with the results of Haaland et al. (2008, 2009), this corresponds to positive  $V_y$  values for the lunar ions in the southern lobes, as panel (b) shows. The other event in the southern lobe has a positive IMF  $B_y$ , which may be due to the relatively rapid variation of the IMF  $B_z$  and the influence of the stronger dynamic pressure of solar wind. As described by Haaland et al. (2008), both of these two factors could affect the dawn-dusk convection in the lobes. Panel (l) shows the north-south component of IMF for each event, which may affect the occurrence of magnetopause reconnection. In order to more quantitatively study the influence of different factors on the plasma convection of tail lobes, we will investigate the correlation of each factor with the motion of lunar ions in the next section.

The measurement shows that the trajectories of the ARTEMIS probes are mostly located within  $\pm 0.5 R_E$  in the Z direction. The highest  $V_x$  is correlated with positions close to the SSE x axis, where ambient field lines are most likely to intersect the lunar surface and allow lunar pick up ions to stream earthward after interacting with the lunar photoelectron sheath. The events in the southern lobe are located near, above and below the lunar equator respectively, and the events in the northern lobe are almost equally distributed in latitude. The largest magnetospheric activity occurred during the southern lobe events.

### 3. Correlation With Upstream Conditions and Magnetospheric Activity

As described in the introduction, the upstream solar wind conditions and magnetospheric activity can affect the plasma convection in the magnetotail lobes. However, the situation for the magnetotail lobes near the Moon  $\sim 60 R_E$  downstream from the Earth has been insufficiently studied. In this section, we statistically investigate the correlation between solar wind conditions and the plasma convection in the deep lobes, as inferred from the lunar ion velocity.

In order to calculate the correlation coefficients between the lunar ion velocities and the upstream parameters, we interpolated the lunar ion velocity to 1-min time resolution in order to correspond to the time resolution of the upstream parameters from OMNI data set. In addition, because there were only three events measured in the southern lobe, we converted these measurements to the corresponding parameters

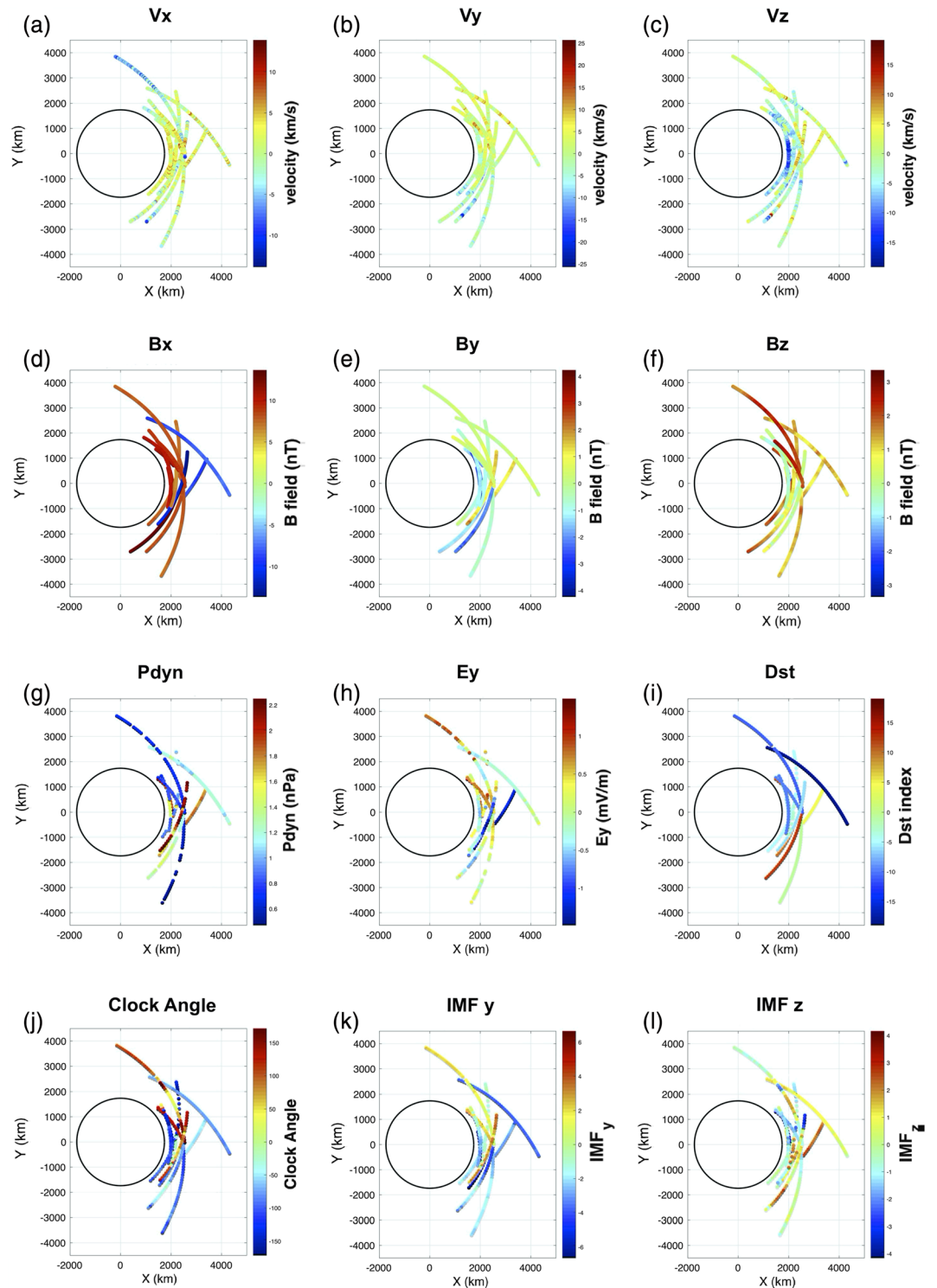


**Figure 1.** (a–l) ARTEMIS measurements of lunar ions and ambient magnetic fields, and synchronous measurements of upstream conditions, including the solar wind dynamic pressure, the dawn-dusk component of electric field, the lateral components of IMF and its clock angle, and the magnetospheric activity: the Dst index. All parameters are mapped along the trajectories of the ARTEMIS probes in the SSE  $XY$  plane.



**Table 1**  
The Correlation Matrix Between the Upstream Conditions and the Lateral Components of the Lunar Ion Velocity

	Pdyn	Ey	IMF_y	IMF_z	Dst	ClockAngle	Lobe_Bx	Lobe_By	Lobe_Vy	Lobe_Vz
Pdyn	1.000	-0.437	-0.014	0.004	0.308	0.015	-0.421	-0.004	-0.167	-0.262
Ey	-0.437	1.000	0.408	-0.788	-0.171	0.247	0.471	-0.194	0.418	0.028
IMF_y	-0.014	0.408	1.000	-0.374	-0.096	0.820	-0.028	0.419	0.494	0.040
IMF_z	0.004	-0.788	-0.374	1.000	0.023	-0.152	-0.356	0.194	-0.376	0.242
Dst	0.308	-0.171	-0.096	0.023	1.000	-0.128	0.426	-0.474	-0.146	-0.292
ClockAngle	0.015	0.247	0.820	-0.152	-0.128	1.000	-0.062	0.405	0.426	0.144
Lobe_Bx	-0.421	0.471	-0.028	-0.356	0.426	-0.062	1.000	-0.711	-0.189	-0.566
Lobe_By	-0.004	-0.194	0.419	0.194	-0.474	0.405	-0.711	1.000	0.307	0.597
Lobe_Vy	-0.167	0.418	0.494	-0.376	-0.146	0.426	-0.189	0.307	1.000	-0.078
Lobe_Vz	-0.262	0.028	0.040	0.242	-0.292	0.144	-0.566	0.597	-0.078	1.000

*Note.* The colored cells represent the correlation coefficients between each of upstream conditions and the  $V_y$  and  $V_z$  of the lunar ions. Red colors indicate larger correlations and blue colors indicate larger anticorrelations. For correlations with upstream and magnetospheric activity indices, the lateral components of the lunar ion velocity in the southern lobe ( $B_x < 0$ ) are flipped, as described in the text. For correlations between the lateral components of the velocity and the lobe magnetic fields, the lateral components of the lunar ion velocity are not flipped.

expected in the northern lobe by flipping the sign of the  $V_y$  and  $V_z$  components of these southern lobe events. As previous studies showed both  $V_y$  and  $V_z$  are oppositely oriented in northern and southern lobes (Haaland et al., 2008, 2009), the convection should be approximately 180° rotated between the two tail lobes.

The correlation matrix in Table 1 shows the correlation coefficients between each of the upstream parameters and the lateral velocity components of the lunar ions measured by ARTEMIS. The lobe field  $B_x$  has the largest anticorrelation ( $-0.566$ ) with  $V_z$ , which indicated  $V_z$  is strongly related to  $B_x$ . The high degree of anticorrelation is probably due to the basic mechanics of the global convection of the magnetosphere, for example, Dungey Cycle. In particular, during periods of greater reconnection or solar wind driving, the overall Dungey Cycle speeds up (e.g.,  $V_z$  in the lobes increases), and magnetic fields pile up more, therefore  $B_x$  in the lobes becomes stronger. This is consistent very well with the fact that the convecting plasma in the lobes moves toward the central plasma sheet from the two different hemispheres. The correlation coefficients between  $V_z$  and IMF  $B_y$ , clock angle, and  $E_y$  are much less significant than for  $V_y$ . This is probably related to the fact that the ARTEMIS measurements are located near the equatorial plane and thus the lunar ions do not have a chance to accelerate as much in the  $Z$  direction. The north-south component of plasma convection in the lobes ( $V_z$ ) has different driving parameters from that of  $V_y$ . For instance, Dst index shows a smaller anticorrelation with  $V_y$  ( $-0.146$ ) compared to  $-0.292$  with  $V_z$ . The correlation between lobe  $B_y$  and  $V_z$  has also a relatively high value. This might be because of field line draping and/or warping around the lunar ionosphere as the convecting magnetotail field lines try to pass by the Moon, or due to the underlying anticorrelation between the lobe  $B_x$  and  $B_y$  resulting from the tail axis shifted from the Sun-Earth line by the solar wind aberration.

The correlation between the lunar ion  $V_y$  and the IMF  $B_y$  has a relatively high value ( $\sim 0.5$ ). This is consistent with previous observations that showed that the dawn-dusk convection in the tail lobes is strongly influenced by the IMF  $B_y$  (Haaland et al., 2008). The IMF  $B_y$  component is associated with the field geometry of the upstream interaction with the solar wind, which can affect the asymmetry of the convection in the magnetosphere (Tenfjord et al., 2015). The correlation between  $V_y$  and IMF clock angle is relatively significant (0.426) as well, which is expected since clock angle is highly correlated with  $B_y$ . In addition, we found that the correlation between  $V_y$  and  $E_y$  is also relatively significant, which has not been reported before. This may occur because the dawn-dusk component of the solar wind electric field drives the lateral flux tubes to the nightside of the Earth, which might be linked to upstream reconnection.

#### 4. Summary

In general, the lunar ion data from ARTEMIS and the upstream condition data from the OMNI data set appear very consistent with previous studies of the convection of the tail lobes closer to the Earth

(Haaland et al., 2008, 2009; Ohma et al., 2019). This suggests that measurements of lunar ions provide a useful tool to investigate the convection in the deep lobes near the orbital distance of the Moon in the magnetotail. The ARTEMIS and OMNI data demonstrate that the convection in the deep tail is influenced by the upstream parameters and magnetospheric activity. The IMF  $B_y$  and clock angle have significant correlations with the inferred convection in the deep tail, as predicted. In addition, the dawn-dusk component of the interplanetary electric field may significantly affect the convection in the lobes. This correlation should be addressed in future studies, as it may represent a link between dayside reconnection and magnetospheric convection. The limitation of this method is that this technique needs the existence of a heavy ion source to calculate and estimate the tenuous ambient plasma velocity. The background ion density should be much smaller than the lunar heavy ion density during the period when lunar ions were detected. However, the method of using lunar ions to measure the magnetospheric convection could be potentially applied to moons of other planetary system objects when the ambient plasma cannot be directly measured.

### Data Availability Statement

All ARTEMIS data are publicly available at NASA's CDAWeb (<https://cdaweb.sci.gsfc.nasa.gov>) and the ARTEMIS site (<http://artemis.ssl.berkeley.edu>).

### Acknowledgments

We acknowledge support from the Solar System Exploration Research Virtual Institute, Lunar Data Analysis Program grant 80NSSC20K0311, and NASA contract NAS5-02099. We acknowledge James P McFadden for Electrostatic Analyzer data. We acknowledge the OMNI data, which were obtained from the GSFC/SPDF OMNIWeb interface (at <https://omniweb.gsfc.nasa.gov>).

### References

- Angelopoulos, V. (2011). The ARTEMIS Mission. *Space Science Reviews*, *1*(165), 3–25.
- Auster, H. U., Glassmeier, K. H., Magnes, W., Aydogar, O., Baumjohann, W., Constantinescu, D., et al. (2008). The THEMIS fluxgate magnetometer. *Space Science Reviews*, *141*(1–4), 235–264. <https://doi.org/10.1007/s11214-008-9365-9>
- Cao, X., Halekas, J., Poppe, A., Chu, F., & Glassmeier, K. H. (2020). The acceleration of lunar ions by magnetic forces in the terrestrial magnetotail lobes. *Journal of Geophysical Research: Space Physics*, *125*, e2020JA027829. <https://doi.org/10.1029/2020JA027829>
- Cook, J. C., Stern, S. A., Feldman, P. D., Gladstone, G. R., Retherford, K. D., & Tsang, C. C. (2013). New upper limits on numerous atmospheric species in the native lunar atmosphere. *Icarus*, *225*(1), 681–687. <https://doi.org/10.1016/j.icarus.2013.04.010>
- Cowley, S. W. H. (1981). Magnetospheric asymmetries associated with the Y-component of the IMF. *Planetary and Space Science*, *29*(1), 79–96. [https://doi.org/10.1016/0032-0633\(81\)90141-0](https://doi.org/10.1016/0032-0633(81)90141-0)
- Cowley, S. W. H., & Lockwood, M. (1992). Excitation and decay of solar wind-driven flows in the magnetosphere-ionosphere system. *AnGeo*, *10*(1–2), 103–115.
- Haaland, S., Lybekk, B., Svenes, K., Pedersen, A., Förster, M., Vaith, H., & Torbert, R. (2009). Plasma transport in the magnetotail lobes. *Annales Geophysicae*, *27*(9), 3577–3590. <https://doi.org/10.5194/angeo-27-3577-2009>
- Haaland, S., Paschmann, G., Förster, M., Quinn, J., Torbert, R., Vaith, H., et al. (2008). Plasma convection in the magnetotail lobes: Statistical results from Cluster EDI measurements. *Annales Geophysicae*, *26*(8), 2371–2382.
- Halekas, J. S., Delory, G. T., Farrell, W. M., Angelopoulos, V., McFadden, J. P., Bonnell, J. W., et al. (2011). First remote measurements of lunar surface charging from ARTEMIS: Evidence for nonmonotonic sheath potentials above the dayside surface. *Journal of Geophysical Research*, *116*, A07103. <https://doi.org/10.1029/2011JA016542>
- Halekas, J. S., Poppe, A. R., Delory, G. T., Sarantos, M., Farrell, W. M., Angelopoulos, V., & McFadden, J. P. (2012). Lunar pickup ions observed by ARTEMIS: Spatial and temporal distribution and constraints on species and source locations. *Journal of Geophysical Research*, *117*, E06006. <https://doi.org/10.1029/2012JE004107>
- Halekas, J. S., Poppe, A. R., Delory, G. T., Sarantos, M., & McFadden, J. P. (2013). Using ARTEMIS pickup ion observations to place constraints on the lunar atmosphere. *Journal of Geophysical Research: Planets*, *118*, 81–88. <https://doi.org/10.1029/2012JE004292>
- Halekas, J. S., Poppe, A. R., Harada, Y., Bonnell, J. W., Ergun, R. E., & McFadden, J. P. (2018). A tenuous lunar ionosphere in the geomagnetic tail. *Geophysical Research Letters*, *45*, 9450–9459. <https://doi.org/10.1029/2018GL079936>
- Hartle, R. E., & Killen, R. (2006). Measuring pickup ions to characterize the surfaces and exospheres of planetary bodies: Applications to the Moon. *Geophysical Research Letters*, *33*, L05201. <https://doi.org/10.1029/2005GL024520>
- Horányi, M., Szalay, J. R., Kempf, S., Schmidt, J., Grün, E., Srama, R., & Sternovsky, Z. (2015). A permanent, asymmetric dust cloud around the Moon. *Nature*, *522*(7556), 324–326. <https://doi.org/10.1038/nature14479>
- Huebner, W. F., & Mukherjee, J. (2015). Photoionization and photodissociation rates in solar and blackbody radiation fields. *Planetary and Space Science*, *106*, 11–45. <https://doi.org/10.1016/j.pss.2014.11.022>
- Khurana, K. K., Walker, R. J., & Ogino, T. (1996). Magnetospheric convection in the presence of interplanetary magnetic field By: A conceptual model and simulations. *Journal of Geophysical Research*, *101*(A3), 4907–4916. <https://doi.org/10.1029/95JA03673>
- King, J. H., & Papitashvili, N. E. (2005). Solar wind spatial scales in and comparisons of hourly Wind and ACE plasma and magnetic field data. *Journal of Geophysical Research*, *110*, A02104. <https://doi.org/10.1029/2004JA010649>
- Lin, R. P., Anderson, K. A., McCoy, J. E., & Russell, C. T. (1977). Observations of magnetic merging and the formation of the plasma sheet in the Earth's magnetotail. *Journal of Geophysical Research*, *82*(19), 2761–2773. <https://doi.org/10.1029/JA082i019p02761>
- McCoy, J. E., Anderson, K. A., Lin, R. P., Howe, H. C., & McGuire, R. E. (1975). Lunar remnant magnetic field mapping from orbital observations of mirrored electrons. *The moon*, *14*(1), 35–47. <https://doi.org/10.1007/BF00562971>
- McFadden, J. P., Carlson, C. W., Larson, D., Ludlam, M., Abiad, R., Elliott, B., et al. (2008). The THEMIS ESA plasma instrument and in-flight calibration. *Space Science Reviews*, *141*(1–4), 277–302. <https://doi.org/10.1007/s11214-008-9440-2>
- McGrath, M. A., Johnson, R. E., & Lanzerotti, L. J. (1986). Sputtering of sodium on the planet Mercury. *Nature*, *323*(6090), 694–696. <https://doi.org/10.1038/323694a0>

- Ohma, A., Østgaard, N., Reistad, J. P., Tenfjord, P., Laundal, K. M., Moretto Jørgensen, T., et al. (2019). Observations of asymmetric lobe convection for weak and strong tail activity. *Journal of Geophysical Research: Space Physics*, *124*, 9999–10,017. <https://doi.org/10.1029/2019JA026773>
- Poppe, A. R., Samad, R., Halekas, J. S., Sarantos, M., Delory, G. T., Farrell, W. M., et al. (2012). ARTEMIS observations of lunar pick-up ions in the terrestrial magnetotail lobes. *Geophysical Research Letters*, *39*, L17104. <https://doi.org/10.1029/2012GL052909>
- Sarantos, M., Hartle, R. E., Killen, R. M., Saito, Y., Slavin, J. A., & Glocer, A. (2012). Flux estimates of ions from the lunar exosphere. *Geophysical Research Letters*, *39*, 13101. <https://doi.org/10.1029/2012GL052001>
- Sarantos, M., Killen, R. M., Glenar, D. A., Benna, M., & Stubbs, T. J. (2012). Metallic species, oxygen and silicon in the lunar exosphere: Upper limits and prospects for LADEE measurements. *Journal of Geophysical Research*, *117*, A03103. <https://doi.org/10.1029/2011JA017044>
- Stern, S. A. (1999). The lunar atmosphere: History, status, current problems, and context. *Reviews of Geophysics*, *37*(4), 453–491. <https://doi.org/10.1029/1999RG900005>
- Tenfjord, P., Østgaard, N., Snekvik, K., Laundal, K. M., Reistad, J. P., Haaland, S., & Milan, S. E. (2015). How the IMF By induces a By component in the closed magnetosphere and how it leads to asymmetric currents and convection patterns in the two hemispheres. *Journal of Geophysical Research: Space Physics*, *120*, 9368–9384. <https://doi.org/10.1002/2015JA021579>
- Troshichev, O., Kokubun, S., Kamide, Y., Nishida, A., Mukai, T., & Yamamoto, T. (1999). Convection in the distant magnetotail under extremely quiet and weakly disturbed conditions. *Journal of Geophysical Research*, *104*(A5), 10,249–10,263. <https://doi.org/10.1029/1998JA900141>
- Vorburger, A., Wurz, P., Barabash, S., Wieser, M., Futaana, Y., Holmström, M., et al. (2014). First direct observation of sputtered lunar oxygen. *Journal of Geophysical Research: Space Physics*, *119*, 709–722. <https://doi.org/10.1002/2013JA019207>
- Zhou, X. Z., Angelopoulos, V., Poppe, A. R., & Halekas, J. S. (2013). ARTEMIS observations of lunar pickup ions: Mass constraints on ion species. *Journal of Geophysical Research: Planets*, *118*, 1766–1774. <https://doi.org/10.1002/jgre.20125>